Thrombin-Responsive Transcutaneous Patch for Auto-Anticoagulant Regulation

Yuqi Zhang, Jicheng Yu, Jinqiang Wang, Nicholas J. Hanne, Zheng Cui, Chenggen Qian, Chao Wang, Hongliang Xin, Jacqueline H. Cole, Caterina M. Gallippi, Yong Zhu,* and Zhen Gu**

Thrombosis, a pathological hemostatic condition, has become one of the leading causes of cardiovascular mortalities and morbidities worldwide.[1,2] The unwanted intravascular blood thrombi can cause vascular occlusions, organ damage, and severe cardiovascular diseases, including myocardial infarction and stroke.[3] As a first line of defense, anticoagulant drugs can prevent and delay the obstruction in blood flow.[2,4] Heparin (HP), a common anticoagulant, is routinely administered to counteract coagulation activation.[5] Dosing schemes for HP usually involve daily intravenous administration for weeks to months.[6] Unfortunately, systemic (intravenous) or local (catheter) delivery of anticoagulants remains difficult for precise anticoagulant regulation.[7] Under- or over-dosage may lead to dangerous consequences due to either rapid clearance in the body or bleeding complications that may lead to spontaneous hemorrhages.[8] Moreover, it is known that the timely delivery of drugs is critical for cardiovascular patients when an unpredictable attack happens,[9] which makes sustained protection from pathogenesis imperative. Therefore, a controlled and on-demand drug delivery system, one that enhances therapeutic efficacy while minimizing side effects and time–to–treatment, is urgently needed for the management of thrombotic diseases.[10]

Herein, we report an engineered feedback-controlled anticoagulant system based on thrombin-responsive polymer–drug conjugates. Thrombin is a trypsin-like serine proteinase that plays an imperative role in blood coagulation systems to produce insoluble fibrin from soluble fibrinogen.[11] Recently, thrombin-responsive systems based on the thrombin-cleavable peptide have attracted great attention due to associated high sensitivity and fast response rate.[12] In our system, a thrombin-cleavable peptide is introduced as a linker during the conjugation of HP to the main chain of hyaluronic acid (HA).[13] The peptide can be cleaved when thrombin is activated,[14,15] triggering drug release from the backbone in a thrombin-responsive fashion (**Figure 1**a). The thrombin-responsive HP conjugated HA (TR-HAHP) matrix can be obtained via polymerization under ultraviolet (UV) light treatment. In the presence of the elevated thrombin concentration, HP can be promptly released from the TR-HAHP matrix, whereas HP is trapped in the matrix and cannot be released without thrombin. The released HP is able to inhibit the coagulation activation by inactivating thrombin, which suppresses the release of HP from the matrix and minimizes the risk of undesirable spontaneous hemorrhage.

The TR-HAHP derivative can be further integrated into a disposable microneedle (MN) array based transcutaneous device for potential long-term autoregulation of blood coagulation. The micro-size needles on the patch enable convenient administration in a painless manner.[16,17] Owing to the thrombin-responsive property, this MN patch acts as a closed-loop "smart" device that can be safely inserted in the skin without drug leaking under a normal blood environment, but rapidly responds to an increased thrombin level and releases a corresponding dose of anticoagulant drug to prevent the undesired formation of blood clots (Figure 1b). We demonstrate that this "smart" HP patch can offer sustained autoregulation of blood coagulation in a safe and convenient manner.

To achieve the stimuli-triggered heparin delivery, a thrombin cleavable peptide with a sequence of GGLVPR|GSGGC, was introduced as a linker to obtain the TR-HAHP. The cleavage of the peptide by thrombin was verified by liquid chromatography mass spectrometry (LCMS) analysis, which showed that the peptides were efficiently cleaved after 12 h incubation with 1 U mL^{-1} thrombin in Tris buffer (20×10^{-3} M Tris, 150×10^{-3} M NaCl, 2.5×10^{-3} M KCl, pH 7.4) (Figure S1, Supporting Information).

Y. Zhang, J. Yu, Dr. J. Wang, N. J. Hanne, C. Qian, Dr. C. Wang, Prof. H. Xin, Prof. J. H. Cole, Prof. C. M. Gallippi, Prof. Y. Zhu, Prof. Z. Gu
Joint Department of Biomedical Engineering
University of North Carolina at Chapel Hill
and North Carolina State University
Raleigh, NC 27695, USA
E-mail: cmgallip@email.unc.edu; yong_zhu@ncsu.edu; zgu@email.unc.edu

Y. Zhang, J. Yu, Dr. J. Wang, Dr. C. Wang, Prof. Z. Gu
Center for Nanotechnology in Drug Delivery and Division of Molecular Pharmaceutics
UNC Eshelman School of Pharmacy
University of North Carolina at Chapel Hill
Chapel Hill, NC 27599, USA

Z. Cui, Prof. Y. Zhu
Department of Mechanical and Aerospace Engineering
North Carolina State University
Raleigh, NC 27695, USA

Prof. H. Xin
School of Pharmacy
Nanjing Medical University
Nanjing 211166, China

Prof. Z. Gu
Department of Medicine
University of North Carolina at Chapel Hill
Chapel Hill, NC 27599, USA

DOI: 10.1002/adma.201604043

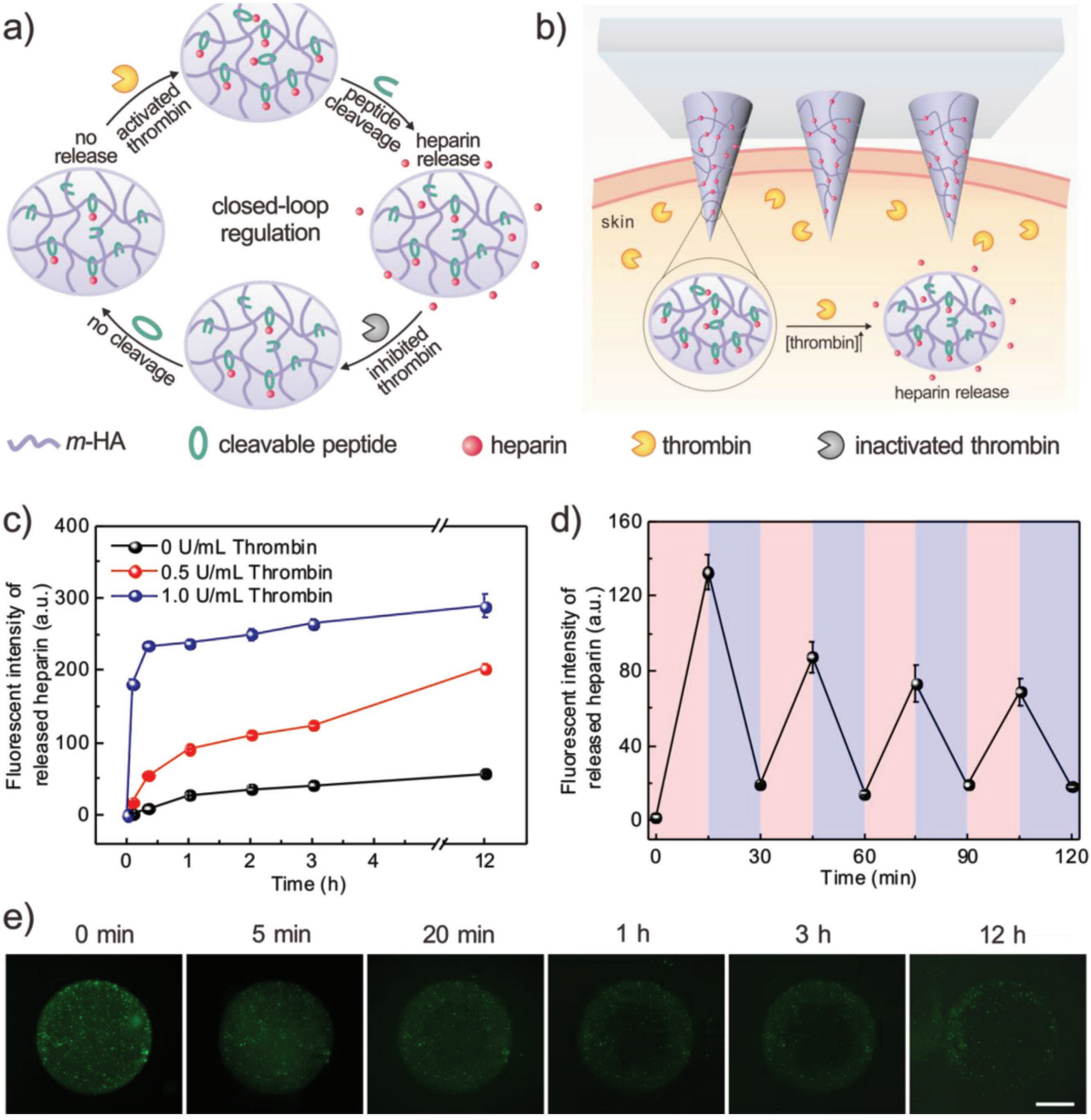

Figure 1. a) Formation and mechanism of the feedback-controlled heparin delivery system based on thrombin-responsive HAHP (TR-HAHP) conjugate. b) Schematic of the TR-HAHP MN array patch in response to thrombin. c) In vitro accumulated FITC-labeled HP release from the TR-HAHP hydrogel in several thrombin concentrations at 37 °C. d) Pulsatile release profile of FITC-HP from the TR-HAHP hydrogel (blue: w/o thrombin; pink: w/ thrombin). e) Fluorescence microscopy images of the TR-HAHP hydrogel in thrombin solution at indicated time points. Scale bar: 1 mm. Error bars indicate s.d. ($n = 3$).

To prepare the TR-HAHP, the cleavable peptide was first conjugated to the methacrylated HA (m-HA) through the formation of an amide bond. Then, HP was further covalently bound to the cysteine residue of the peptide to obtain the TR-HAHP. In the presence of the activated thrombin, the short peptide can be selectively recognized and cleaved between Arg (R) and Gly (G) to achieve specific HP release.[14] The successful conjugation of HP to m-HA was evidenced by the elemental analysis and the increase in molecular weight from 314 to 606 kDa (Table S1, Supporting Information).

In order to examine the effect of thrombin in the TR-HAHP based system, a TR-HAHP hydrogel was prepared via photo-polymerization (Figure S2, Supporting Information). The prepared hydrogels were incubated in thrombin solutions with different concentrations (0, 0.5, and 1 U mL^{-1}), and the release kinetics were obtained by measuring the fluorescence

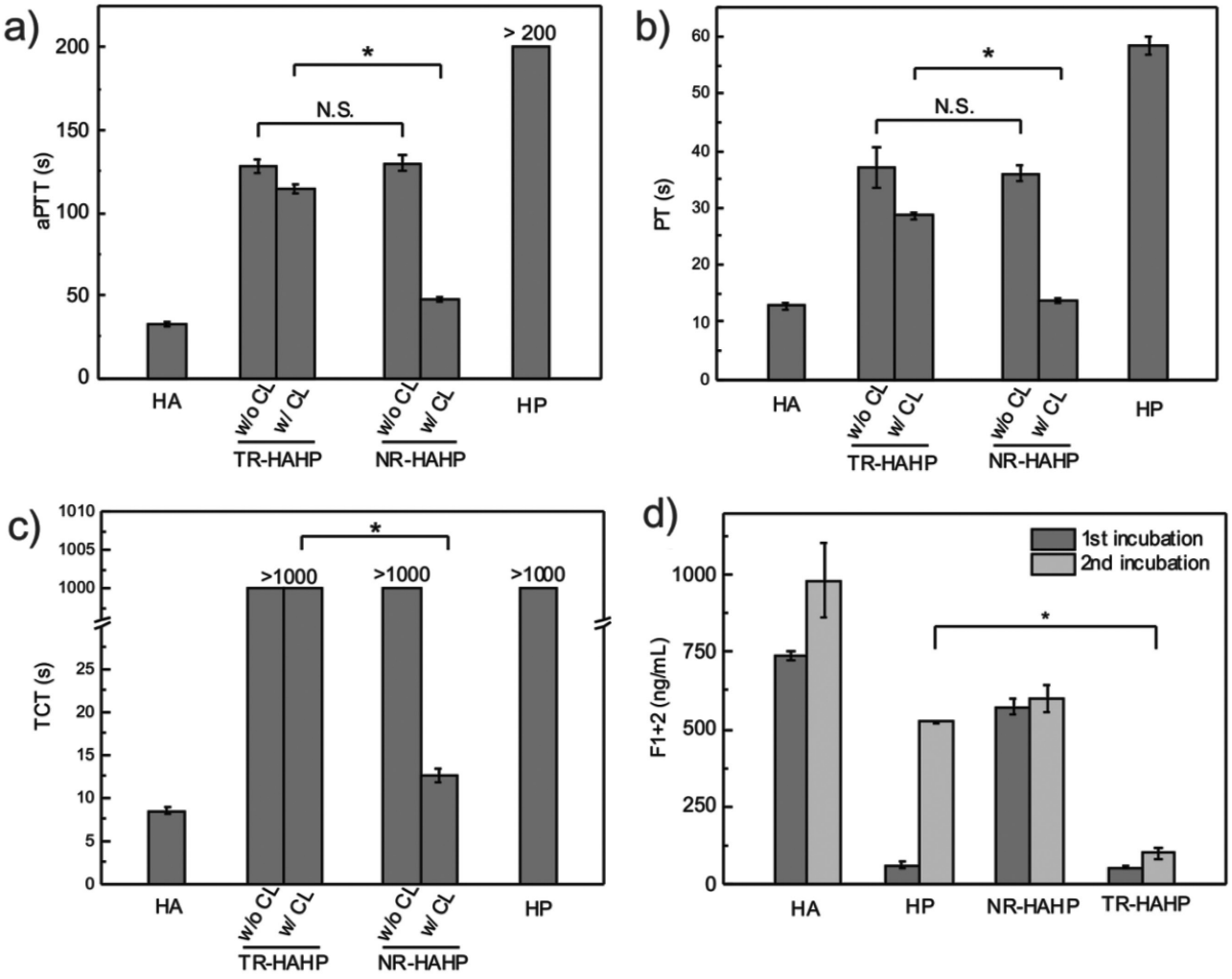

Figure 2. In vitro anticoagulant capacity of the TR-HAHP hydrogel. a) In vitro analysis of the activated thromboplatin time (aPTT) of untreated (HA), HP treated, non-cross-linked, and cross-linked TR-HAHP or NR-HAHP treated plasma. b) Prothrombin time (PT) tests of plasma incubated with HA, HP, TR-HAHP, and NR-HAHP hydrogels. c) Thrombin clotting time (TCT) of plasma added with various hydrogels. d) Concentrations of F1+2 fragment after each incubation period (3 h) indicates that only the TR-HAHP hydrogel can effectively suppress the thrombin generation during the second incubation. Error bars indicate s.d. ($n = 3$).

intensity of FITC-labeled HP. As shown in **Figure 2**a, the release profiles presented a high dependence on the thrombin level. The TR-HAHP hydrogel quickly responded to the relative higher thrombin concentration (1 U mL^{-1}), and released most of the conjugated HP within 20 min, allowing for fast action of the drug under urgent clinical situations. In contrast, the hydrogel was stable in the buffer without thrombin for up to 12 h (Figure 1c and Figure S3, Supporting Information). Furthermore, a pulsatile release pattern was observed when the TR-HAHP hydrogel was alternately exposed every 15 min for several cycles to solutions with and without thrombin (Figure 1d). The hydrogel performed the repeatable and sustained release of HP, corresponding to the presence or absence of thrombin. Additionally, the release process was monitored in real time by fluorescence microscopy. As demonstrated in Figure 1e, the cleaved FITC-HP gradually diffused through the cross-linked hydrogel after the addition of thrombin, while the hydrogel maintained its original structure during the release period. In contrast, there was insignificant fluorescence signal detected in the buffer without thrombin after 12 h (Figure S3, Supporting Information). To further confirm the thrombin-responsive release, a non-responsive HP-HA conjugate without the thrombin-sensitive peptide (NR-HAHP) was synthesized directly via a heterobifunctional linker as a negative control. From the fluorescence images and release profiles of the NR-HAHP hydrogel incubating with thrombin solutions, it was demonstrated that HP could not detach from the HA matrix without the degradation of the thrombin-sensitive peptide (Figures S3 and S4, Supporting Information). Collectively, these results suggested that the thrombin-specific activation feature of the TR-HAHP is attributed to the incorporation of the cleavable peptide unit.

To validate the in vitro anticoagulant regulation ability of TR-HAHP, the activated thromboplatin time (aPTT) and prothrombin time (PT) were measured to determine the anticoagulant potency of different samples, including the empty HA

hydrogel, HA hydrogel containing free HP, TR-HAHP gel, and NR-HAHP gel by incubation with human plasma. The activated thromboplatin time measurement is commonly used for the evaluation of the intrinsic pathways of blood coagulation,[18] while the PT measurement is a test for the evaluation of extrinsic pathways in clinical medicine.[19] Antithrombin III, a natural thrombin inhibitor, can inactivate thrombin via forming a covalent enzyme complex with thrombin.[20] Since it has a specific heparin binding-site proximal to the pentasaccharide, the inactivation of thrombin by antithrombin III can be promoted by nearly three orders of magnitude in the presence of heparin.[21] As shown in Figure 2a,b, compared with the healthy human plasma treated with the empty gel, both TR-HAHP and NR-HAHP solutions prolonged aPTT and PT by up to 100 s. These prolonged aPTT and PT can be attributed to the existence of heparin based on an antithrombin-dependent mechanism.[22] However, once cross-linked by UV irradiation, the NR-HAHP gel could not inhibit the coagulation while the TR-HAHP gel still showed a remarkable increase in the aPTT and PT levels, indicating the thrombin-specific release of HP from the TR-HAHP gel. We further evaluated the anticoagulant capability of the TR-HAHP via a thrombin clotting time (TCT) assay, which is commonly performed on patients for diagnosis of coagulopathy by adding thrombin to citrated plasma and recording the time when a stable clot is formed.[23] Consistent with the aPTT and PT results, TCT was significantly delayed in the presence of the TR-HAHP gel (Figure 2c).

Encouraged by the above findings, we further incubated the hydrogels with human plasma twice with 3 h for each incubation cycle to examine the self-regulation ability of the TR-HAHP. Thrombin formation in plasma was determined by the level of the prothrombin F1+2 fragment, which is cleaved from prothrombin during the activation.[24] The coagulation activation levels of the TR-HAHP hydrogel versus non-responsive gels (HP and NR-HAHP) were reported in Figure 2d. A high level of F1+2 was detected in the plasma incubated with the control groups (HA and NR-HAHP), while both HP gel and the TR-HAHP gel effectively inhibited coagulation activation in the first incubation cycle. In the presence of TR-HAHP hydrogel, plasma was protected from clotting over both investigated periods, whereas plasma in contact with the HP hydrogel could only prevent coagulation in the first incubation cycle due to the burst release of HP from the gel during the incubation. The thrombin responsiveness of the TR-HAHP enabled the controlled and repeatable HP release from the system, as less HP was released once thrombin was inhibited by the pre-released HP. The remarkable difference in F1+2 concentrations between plasmas incubated with the HP gel versus the TR-HAHP gel confirmed that the feedback system could inhibit coagulation over a long time period, as expected.

To achieve a functional form that enables painless and convenient HP delivery, we next fabricated a TR-HAHP MN array patch to assess long-term anticoagulant regulation. Briefly, the TR-HAHP solution mixed with the cross-linker MBA and a

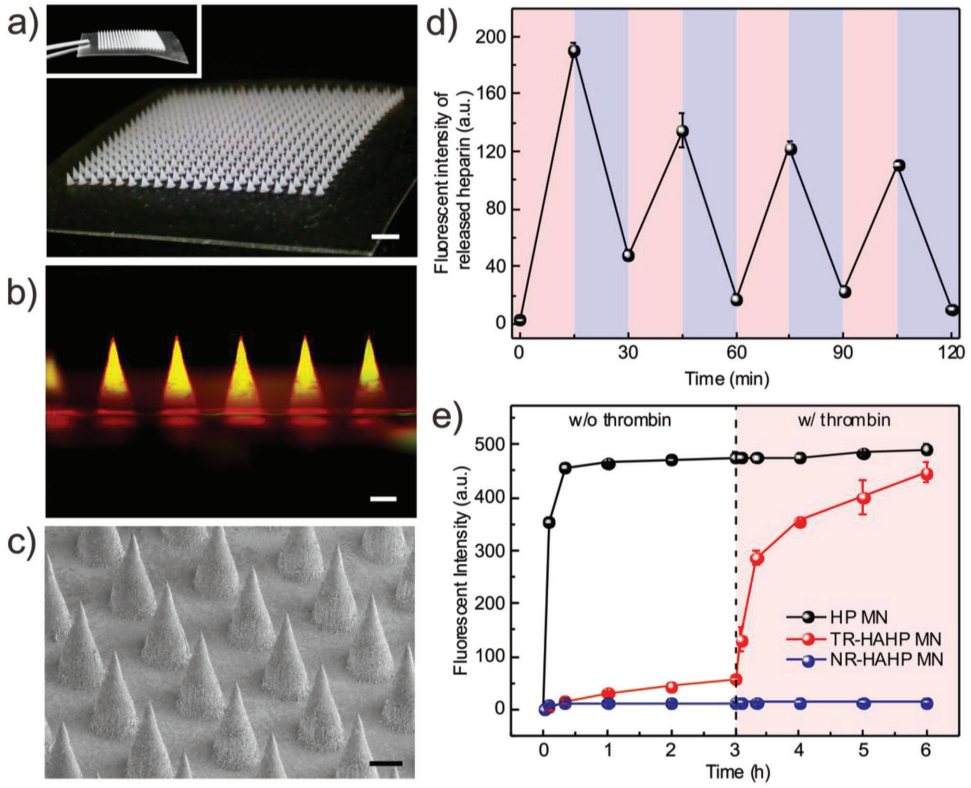

Figure 3. Fabrication and in vitro characterization of the TR-HAHP MN array patch. a) Photos of the MNs array. Scale bar: 1 mm. b) A fluorescence microscopy image of rhodamine-labeled MN loaded with FITC-labeled TR-HAHP. Scale bar: 200 µm. c) A SEM image of MNs. Scale bar: 200 µm. d) Pulsatile release profile of FITC-HP from the TR-HAHP MNs. (blue: w/o thrombin; pink: w/ thrombin). e) Self-regulated FITC-HP release from MNs in different thrombin solutions. Error bars indicate s.d. ($n = 3$).

photoinitiator was first loaded into the tip region of a silicone MN mold by centrifugation. The cross-linked HA-based matrix enhances the stiffness of the MNs (Figure S5, Supporting Information) for efficient penetration through the skin,[16] as well as restricts the loss of the TR-HAHP from the MNs. The MN array contains 400 needles in a 12 × 12 mm^2 patch with a 600 µm center-to-center interval (**Figure 3**a). Each MN was of a conical shape, with 300 µm in diameter at the base and 600 µm in height (Figure 3c). The fluorescence image in Figure 3b displayed a cross-sectional view of the MN with a rhodamine-labeled m-HA matrix and FITC-labeled TR-HAHP loaded in MN tips with a homogenous distribution.

The obtained TR-HAHP MNs exhibited thrombin-responsive performance similar to the TR-HAHP hydrogel. As shown in Figure 3d, a repeatable release profile of HP was observed corresponding to thrombin levels, which may further enable prolonged thrombin-mediated HP delivery. In addition, tunable release kinetics can be achieved by varying the incubating condition (Figure 3e). A maximum of a 15.6-fold increase in the HP release rate was observed in 20 min once exposed to thrombin solution (0.6 U mL^{-1}). In contrast, the free HP-loaded MNs exhibited a burst release in the Tris buffer even without thrombin, but an insignificant amount of HP was released from the NR-HAHP MNs.

To further evaluate the potential clinical relevance for the treatment of life-threatening acute thrombosis, we next verified the anticoagulant capacity of the TR-HAHP in a thrombotic challenge model.[25] The CD-1 mice were randomly divided into five groups (n = 8), with one group intravenously (i.v.) injected with heparin solution and four groups transcutaneously administered with different samples: 1) the empty HA MN made of only cross-linked m-HA, 2) the HA MN encapsulating free HP (HP MN), 3) the TR-HAHP MN, and 4) the NR-HAHP MN (HP dose: 200 U kg^{-1}). The MNs could penetrate the mouse skin efficiently, as evidenced by the hematoxylin and eosin (H&E) and trypan blue staining of the MN-treated tissue (**Figure 4**a), which allowed the MN tips to be exposed to the blood fluid in vascular-capillary network for real-time sensing

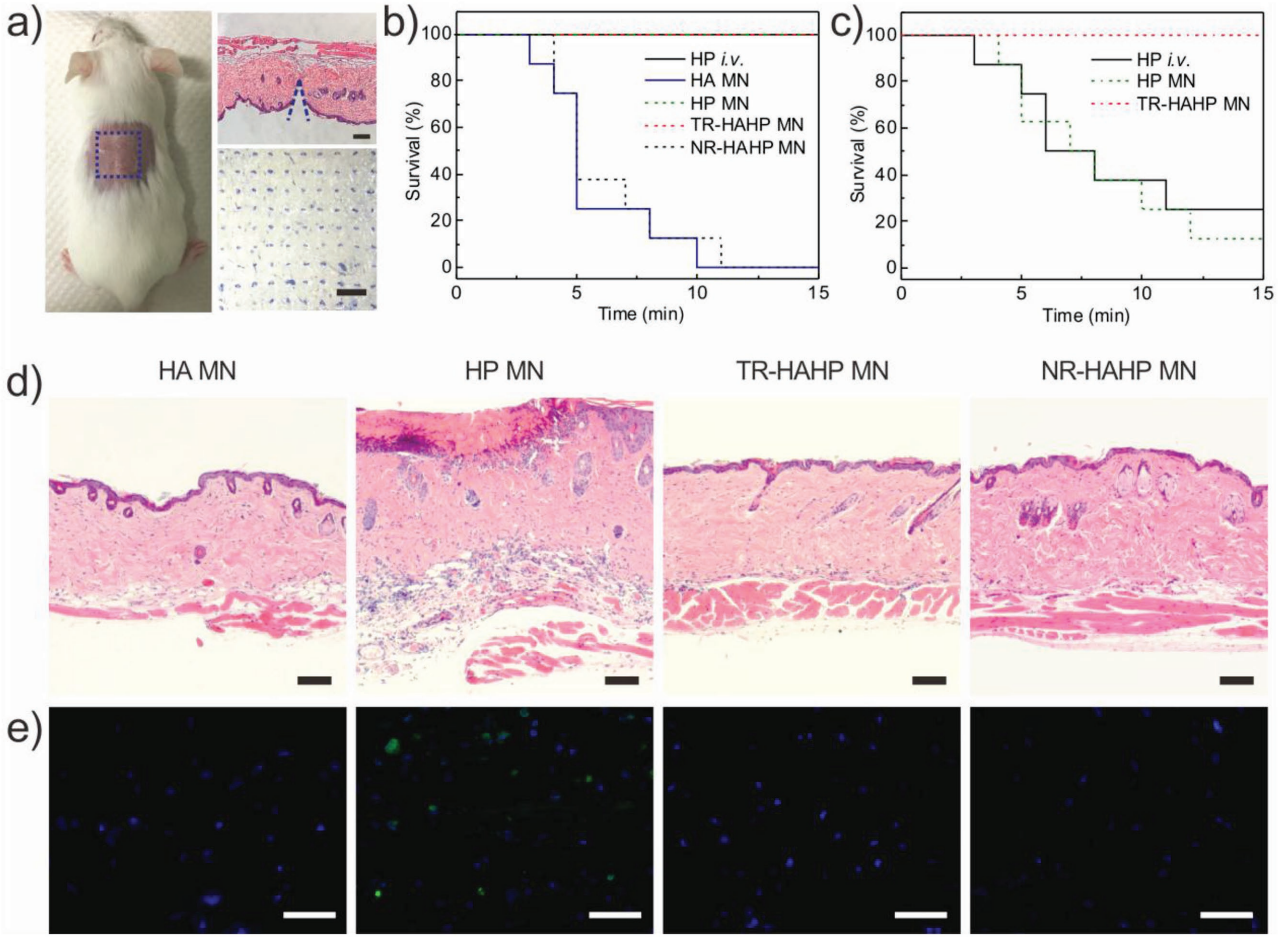

Figure 4. In vivo studies of the TR-HAHP patch for thrombosis preventation. a) Photograph of a mouse transcutaneously administered with the MN array patch (left). H&E-stained microscopy image of mouse skin penetrated by one MN (right top) and the image of the trypan blue staining (right bottom) showing the penetration of the MN patch into the mouse skin. Scale bars are 100 µm and 1 mm, respectively. b) Kaplan–Meier survival curves for the mice challenged with thrombin injection. Each group was pre-treated with HP i.v. injection or different types of the MN patch (HP: 200 U kg^{-1}). Shown are eight mice per treatment group. c) Kaplan–Meier survival curves for thrombotic challenge mouse model 6 h post MN treatments (HP: 200 U kg^{-1}). Shown are eight mice per treatment group. d) H&E-stained sections of mouse skin tissue at the MN-treated sites. Scale bar: 100 µm. e) Immunofluorescence images of mouse skin tissue stained with TUNEL assay (green) and Hoechst (blue). Scale bar: 50 µm.

and rapid response. The transient microchannels in the skin were quickly recovered 4 h post MN injection (Figure S6, Supporting Information).

Each mouse was i.v. injected with thrombin (1000 U kg^{-1}) to induce an acute thromboembolism, which can lead to mortality in ≈92% of mice.[26] Heparin solution was i.v. injected into the mice before thrombosis induction. The MN patches were pre-administered on the dorsum skin of the mice 10 min before the challenge to be tested. All animals with empty HA MN or the NR-HAHP MN died within 15 min after the injection of thrombin, whereas all mice survived with the treatment of HP MN or TR-HAHP MN (Figure 4b) during the 15 min. The significantly enhanced survival rate implied fast and efficient HP release from the TR-HAHP MN in response to increased thrombin, which protected the mice from the thrombolytic risk. Through FITC-labeled heparin, the in vivo release triggered by thrombin was also verified by fluorescence microscopy (Figure S7, Supporting Information). In a further step, we also examined the survival rate 6 h post administration of MN patches and heparin injection. It was demonstrated that ≥80% of mice treated with the HP MNs or i.v. injection of heparin died as a result of the short half-life of HP (≈1 h) (Figure 4c).[27] The increased mortality rate 6 h post administration of HP MNs suggested that the burst release of HP was not able to ensure protection from thrombotic risk. Contrary to the behavior of HP MN, the TR-HAHP MN maintained its function of anticoagulation and protected the animals from death. The superior anticoagulant capacity of TR-HAHP MN was also evidenced by H&E staining of lung sections. There were insignificant differences observed in the lung of mice treated with TR-HAHP MN compared with healthy mice (Figures S8 and S9, Supporting Information); but intravascular and interstitial hemorrhage, blocked blood vessels, and atelectasis were observed in the challenged groups 6 h post administration of HP injection or HP MN (Figure S9, Supporting Information). These data indicate that the stimulus-triggered feature of the TR-HAHP system enables its potential application in self-administered therapy.

To further investigate the biocompatibility of the MN array patches, the mouse skin surrounding the MN-treated area was excised for histological analysis after 24 h administration. The pure HA MN was regarded as a negative control, which exhibited high biocompatibility as observed in the H&E stained histological images (Figure 4d and Figure S10, Supporting Information), whereas obvious damage was observed in the skin treated with HP MN. The H&E images indicated neutrophil infiltration and a severe pathophysiological response because the HP caused subcutaneous bleeding. On the contrary, there were insignificant lesions at the TR-HAHP MN treated site because no HP leaked from the MN in the absence of thrombin. Moreover, as presented in the skin tissues stained with the in situ TUNEL assay, obvious cell apoptosis occurred in the skin treated with HP MN, while no significant cell death was observed in the skin treated with the TR-HAHP MN, NR-HAHP, and pure HA MN (Figure 4e). Finally, the TR-HAHP MN avoided unwanted bleeding due to the locally generated, and considerably lower levels of activated thrombin at the sealing of the major wounds,[28] which could not be sensed by the MNs in the treated subcutaneous tissue (Figure S11, Supporting Information).

In conclusion, we developed a thrombin-responsive patch for auto-regulation of blood coagulation by integrating a TR-HAHP matrix with a MN-array. The thrombin-cleavable peptide unit enabled thrombin-specific activation of drug release from the system with a rate highly dependent on the thrombin concentration. More importantly, it enabled feedback-controlled anticoagulation therapy with minimized risk of over- or underdosage. The in vivo studies in a thrombolytic challenge model demonstrated effective long-term protection from acute pulmonary thromboembolism. Taken together, this work provides a platform for designing closed-loop based drug delivery systems for the treatment of intravascular diseases according to levels of related biomarkers. Moreover, the integration of MNs with stimuli-responsive drug carriers extends the administration methods of therapeutics.[29]

Supporting Information

Supporting Information is available from the Wiley Online Library or from the author.

Acknowledgements

Y.Z. and J.Y. contributed equally to this work. This work was supported by a grant from the Sloan Research Fellowship, NC TraCS, NIH's Clinical and Translational Science Awards (CTSA, NIH Grant No. 1UL1TR001111) at UNC-CH to Z. Gu and by the National Science Foundation (NSF) through ASSIST Engineering Research Center at NC State (EEC-1160483) and EFRI-1240438 to Y. Zhu. The authors acknowledge the use of the Analytical Instrumentation Facility (AIF) at NC State, which was supported by the State of North Carolina and the National Science Foundation (NSF). The strain tests were made using a DTS delaminator supported by the UNC Research Opportunity Initiative. All animals were treated in accordance with the Guide for Care and Use of Laboratory Animals, approved by the Institutional Animal Care and Use Committee (IACUC) of University of North Carolina at Chapel Hill and North Carolina State University.

Received: July 29, 2016
Revised: October 24, 2016
Published online: November 25, 2016

[1] N. Mackman, *Nature* **2008**, *451*, 914.
[2] W. H. Geerts, D. Bergqvist, G. F. Pineo, J. A. Heit, C. M. Samama, M. R. Lassen, C. W. Colwell, *Chest* **2008**, *133*, 381S.
[3] a) B. Engelmann, S. Massberg, *Nat. Rev. Immunol.* **2013**, *13*, 34; b) N. Doshi, J. N. Orje, B. Molins, J. W. Smith, S. Mitragotri, Z. M. Ruggeri, *Adv. Mater.* **2012**, *24*, 3864; c) Q. Hu, C. Qian, W. Sun, J. Wang, Z. Chen, H. N. Bomba, H. Xin, Q. Shen, Z. Gu, *Adv. Mater.* **2016**, DOI:10.1002/adma.201603463.
[4] P. M. Mannucci, M. Franchini, *Ann. Med.* **2011**, *43*, 116.
[5] a) R. Collins, A. Scrimgeour, S. Yusuf, R. Peto, *N. Engl. J. Med.* **1988**, *318*, 1162; b) L. Jin, J. P. Abrahams, R. Skinner, M. Petitou, R. N. Pike, R. W. Carrell, *Proc. Natl. Acad. Sci. USA* **1997**, *94*, 14683.
[6] M. Cohen, C. Demers, E. P. Gurfinkel, A. G. Turpie, G. J. Fromell, S. Goodman, A. Langer, R. M. Califf, K. A. Fox, J. Premmereur, *N. Engl. J. Med.* **1997**, *337*, 447.
[7] M. Moscucci, *J. Invasive Cardiol.* **2002**, *14*, 55B.
[8] P. Prandoni, A. W. Lensing, A. Piccioli, E. Bernardi, P. Simioni, B. Girolami, A. Marchiori, P. Sabbion, M. H. Prins, F. Noventa, *Blood* **2002**, *100*, 3484.

[9] M. J. Davies, A. Thomas, *N. Engl. J. Med.* **1984**, *310*, 1137.
[10] a) N. Korin, M. Kanapathipillai, B. D. Matthews, M. Crescente, A. Brill, T. Mammoto, K. Ghosh, S. Jurek, S. A. Bencherif, D. Bhatta, *Science* **2012**, *337*, 738; b) C. Chen, S. Li, K. Liu, G. Ma, X. Yan, *Small* **2016**, *12*, 4719; c) M. F. Maitz, U. Freudenberg, M. V. Tsurkan, M. Fischer, T. Beyrich, C. Werner, *Nat. Commun.* **2013**, *4*, 2168.
[11] B. Dahlbäck, *Lancet* **2000**, *355*, 1627.
[12] a) R. Bhat, À. Ribes, N. Mas, E. Aznar, F. Sancenón, M. D. Marcos, J. R. Murguía, A. Venkataraman, R. Martínez-Máñez, *Langmuir* **2016**, *32*, 1195; b) C. Argyo, V. Cauda, H. Engelke, J. Rädler, G. Bein, T. Bein, *Chem. Eur. J.* **2012**, *18*, 428.
[13] G. Kogan, L. Šoltés, R. Stern, P. Gemeiner, *Biotechnol. Lett.* **2007**, *29*, 17.
[14] J. Y. Chang, *Eur. J. Biochem.* **1985**, *151*, 217.
[15] R. J. Jenny, K. G. Mann, R. L. Lundblad, *Protein Expression Purif.* **2003**, *31*, 1.
[16] M. R. Prausnitz, R. Langer, *Nat. Biotechnol.* **2008**, *26*, 1261.
[17] a) J. Yu, Y. Zhang, Y. Ye, R. DiSanto, W. Sun, D. Ranson, F. S. Ligler, J. B. Buse, Z. Gu, *Proc. Natl. Acad. Sci. USA* **2015**, *112*, 8260; b) S. P. Sullivan, D. G. Koutsonanos, M. del Pilar Martin, J. W. Lee, V. Zarnitsyn, S.-O. Choi, N. Murthy, R. W. Compans, I. Skountzou, M. R. Prausnitz, *Nat. Med.* **2010**, *16*, 915; c) P. C. DeMuth, Y. Min, B. Huang, J. A. Kramer, A. D. Miller, D. H. Barouch, P. T. Hammond, D. J. Irvine, *Nat. Mater.* **2013**, *12*, 367; d) R. F. Donnelly, T. R. R. Singh, M. J. Garland, K. Migalska, R. Majithiya, C. M. McCrudden, P. L. Kole, T. M. T. Mahmood, H. O. McCarthy, A. D. Woolfson, *Adv. Funct. Mater.* **2012**, *22*, 4879.
[18] a) D. Basu, A. Gallus, J. Hirsh, J. Cade, *N. Engl. J. Med.* **1972**, *287*, 324; b) J. W. Eikelboom, J. Hirsh, *Thromb. Haemostasis* **2006**, *96*, 547.
[19] A. J. Quick, *J. Biol. Chem.* **1935**, *109*, xxiii.
[20] a) R. D. Rosenberg, *N. Engl. J. Med.* **1975**, *292*, 146; b) P. S. Damus, M. Hicks, R. D. Rosenberg, *Nature* **1973**, *246*, 355.
[21] a) J. P. Sheehan, J. E. Sadler, *Proc. Natl. Acad. Sci. USA* **1994**, *91*, 5518; b) J. Hirsh, *N. Engl. J. Med.* **1991**, *324*, 1565.
[22] R. D. Rosenberg, *Am. J. Med.* **1989**, *87*, S2.
[23] V. Ignjatovic, *Haemostasis: Methods Protoc.* **2013**, *992*, 131.
[24] M. Boisclair, D. Lane, H. Philippou, S. Sheikh, B. Hunt, *Thromb. Haemostasis* **1993**, *70*, 253.
[25] S. Momi, G. Nenci, P. Gresele, *Thromb. Res.* **1992**, *65*, S162.
[26] S. Momi, M. Nasimi, M. Colucci, G. G. Nenci, P. Gresele, *Haematologica* **2001**, *86*, 297.
[27] J. Hirsh, W. Van Aken, A. Gallus, C. Dollery, J. Cade, W. Yung, *Circulation* **1976**, *53*, 691.
[28] a) K. E. Brummel, S. G. Paradis, S. Butenas, K. G. Mann, *Blood* **2002**, *100*, 148; b) M. Comer, K. Cackett, S. Gladwell, L. Wood, K. Dawson, *J. Thromb. Haemostasis* **2005**, *3*, 146.
[29] Y. Lu, A. A. Aimetti, R. Langer, Z. Gu, *Nat. Rev. Mater.* **2016**, *1*, 16075.